

HIGH RESOLUTION SPARSE CHANNEL TOMOGRAPHY FOR SLOWLY VARYING ROTATING SXR PROFILES

Hermann Krause, Manfred Kornherr, ASDEX Team, NI Team

IPP Garching, EURATOM Association, Fed. Rep. of Germany

Abstract: A tomographic reconstruction algorithm is presented which allows to reconstruct rotating plasma soft X-ray profiles. The method utilises the fact that the Fourier spectrum of the measured line integrals shows distinct spectral lines of finite width each of which is caused predominantly by one single poloidal harmonic mode. The reconstruction now uses a best-fit method to get for each line the corresponding poloidal harmonic modes. The sum of all modes then is the SXR profile in high poloidal resolution. The nonperfect periodicity of the plasma rotation results in Fourier spectrum lines of finite width. Since the best-fit can be performed for each relevant frequency deviations from periodicity are fully taken into account.

Tokamak plasmas are typically observed by SXR pin-hole cameras the chords of which view the plasma in the same poloidal plane. Tomographic reconstruction methods which do not use plasma rotation [1] then permit a poloidal resolution which depends directly on the number of pin-hole cameras available. For each camera with chords which span across a full plasma diameter one single poloidal harmonic mode can be determined in amplitude and phase. The radial resolution depends on the distance of the camera chords in the plasma. For the typical case of two cameras thus the $M=0$ and the $M=1$ poloidal harmonics can be reconstructed.

If plasma rotation is used a virtually unlimited poloidal resolution is possible even with few cameras. Previous efforts [2] to use plasma rotation required a precise knowledge about the phase angle of the rotating feature as a function of time. This could, in practice, only be determined from inspection of the signals in cases where one single mode with its phase-coupled harmonics was found rotating. Several independently rotating features could thus not be treated.

The new method, in contrast, does not require an explicit information about phase angles. To demonstrate the method a numerical experiment has been conducted. For the geometry of the ASDEX experiment and its two SXR cameras an artificial rotating SXR profile (cf. fig. 1) is assumed. This profile shows on an unvarying base a rotating feature which is predominantly a $M=1$ mode. For a time interval of 1.6 ms the line integrals of 58 chords are calculated by numerical integration. 400 samples at a sampling frequency of 250 kHz are simulated. The rotation frequency is 10 kHz initially and speeds up by 5 percent during the interval. The amplitude of the rotating peak on the base profile grows from zero to a maximum value within the sampling window.

Thus the simulated plasma rotation is nonperiodic due to an unstable rotation speed and an unstable mode amplitude.

Figure 2 shows for a typical chord the calculated line integral (top) and the Fourier spectrum of the signal (bottom). The signal clearly shows the growing mode amplitude. The spectrum is calculated using a standard FFT program the result of which is a discrete spectrum i.e. amplitude and phase are determined for discrete frequencies which span the range from 0 to half the sampling frequency in steps of f_0 given by the inverse of the time window width.

As expected the approximately periodic signal results in distinct lines of finite width. E.g. the line near 10 kHz is caused by the $M=1$ poloidal harmonic, the other lines by the poloidal harmonics $M=2,3,4,\dots$, $M=0$ is centered at small frequencies. Fourier analysis has thus isolated the individual poloidal harmonics from each other.

For tomographic inversion now the plasma profile is represented in polar coordinates as a sum of poloidal harmonics which rotate in both directions at all discrete frequencies (cf. (1)). The radial dependence of the individual cos- and sin-terms is given by a sum over suitable functions. Chosen are modified Zernicke polynomials (cf. (2)). The profile represented is thus determined by the coefficients A_{ilm}^c and A_{ilm}^s which have to be found by a best-fit to the measurements.

$$\epsilon(r, \Theta, t) = \sum_{i=-I}^I \sum_{\ell=0}^L \sum_{m=0}^M (A_{i\ell m}^c \cdot \rho_{\ell m}(r) \cdot \cos(m\Theta - 2\pi i f_0 t) + A_{i\ell m}^s \cdot \rho_{\ell m}(r) \cdot \sin(m\Theta - 2\pi i f_0 t)) \quad (1)$$

$$\rho_{\ell m}(r) = (1 - r^2)^2 \cdot \sum_{s=0}^{\ell} \frac{(-1)^s \cdot (m + 2\ell - s)! \cdot r^{m+2\ell-2s}}{s! \cdot (m + \ell - s)! \cdot (\ell - s)!} \quad (2)$$

The determination of the coefficients splits naturally into separate best-fit problems, one for each discrete frequency since an observed Fourier amplitude at the discrete frequency $i \cdot f_0$ can only be caused by poloidal harmonics which rotate at $i \cdot f_0$ and $-i \cdot f_0$ (cf. (1)). The best-fit is performed to the cos- and sin-amplitudes of the observed Fourier spectrum rather than the observed line integrals directly. The best-fit is a standard linear least-square fit. The fit problem is defined by a matrix whose elements describe the response of one measured channel, i.e. the cos- and sin-amplitudes of the Fourier spectrum at a single discrete frequency due to each of the poloidal harmonic modes with one single radial function at unit intensity. The matrix elements are calculated by numerical integration. Considerable savings are possible since matrix elements are independent of the discrete frequency. Again, the number of cameras determines how many poloidal harmonics with both directions of rotation can be fitted to the measured cos- and sin-amplitude at a discrete frequency.

It is thus necessary to define frequency windows around the observed lines in the Fourier spectra and to assign one poloidal harmonic to each window. In case of window overlap there are discrete frequencies for which two or more modes are assigned. These cases

can still be treated if the number of cameras is larger or equal to the number of modes assigned to a discrete frequency. The process of window setting and mode assignment is a manual input to the process. Obviously window setting is uncritical for narrow lines and difficult for lines which are wider than the line separation. Since line width is determined by deviations from a perfect rigid rotation and line width tends to increase with the higher harmonics there is a practical trade-off between achievable poloidal resolution and how fast the profile of the rotating plasma evolves or how fast the rotation frequency changes.

Figure 3 shows a reconstructed profile to be compared with fig. 1 for the simulated example based on windows 0 to 5 kHz for $M=0$ and 7 kHz to 15kHz for $M=1$. The poloidal resolution is thus chosen to be the same as can be achieved with codes that do not utilise plasma rotation. Obviously poloidal structures are considerably smoothed out. Fig. 4 then gives a reconstruction based on $M=0$ to $M=8$ with suitable windows defined. Here poloidal resolution is drastically improved.

Figure 5 shows a measured signal of an ASDEX discharge and its Fourier spectrum. The signal is sampled at 250 kHz and shows obvious changes in the signal form during the selected time window. Only 29 channels in two cameras were used for the measurement. The spectrum line near 10 kHz is caused by the $M=1$ poloidal harmonic and smaller contributions of $M=2$ to $M=5$ are visible. A reconstruction with suitable windows defined based on $M=0$ to $M=5$ is given in fig. 6.

- [1] R. S. Granetz et al., Nucl. Fusion, 25, p.727, (1985)
 [2] P. Smeulders, IPP-Report 2/252 1983 and Nucl. Fusion 23, p. 529 (1983).

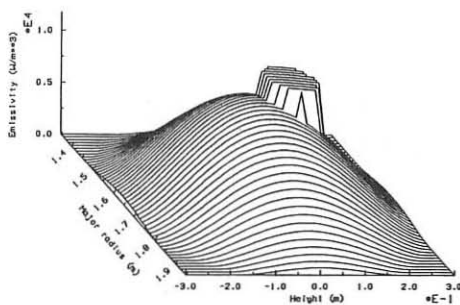


Fig. 1: Simulated SXR profile with rotating peak for $t=1.4$ ms.

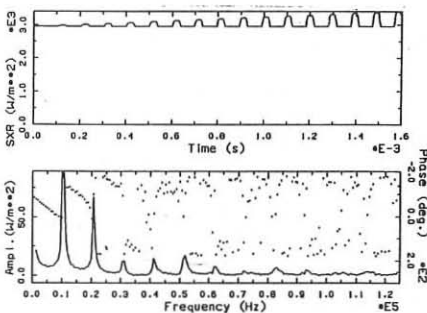


Fig. 2: Calculated SXR line intensity (top) for the rotating profile of fig. 1. Fourier spectrum (bottom) and phases (dotted) of the signal.

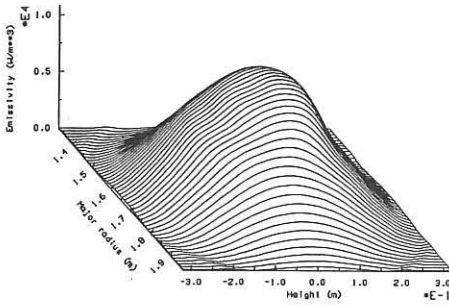


Fig. 3: Reconstruction of the rotating profile of fig. 1 based on $M=0$ and $M=1$ for $t=1.4$ ms.

Fig. 4: Reconstruction of the rotating profile of fig. 1 based on $M=0$ to $M=8$ for $t=1.4$ ms.

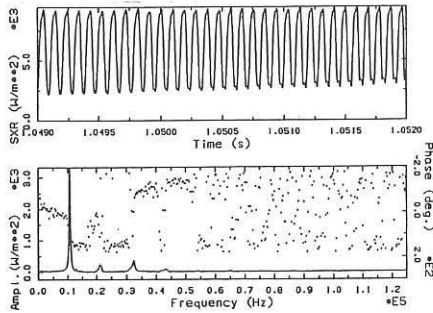
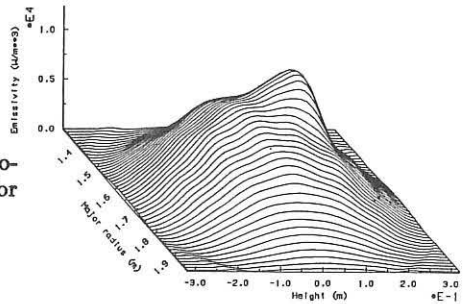


Fig. 5: ASDEX measured SXR signal and Fourier spectrum thereof.

Fig. 6: Reconstruction of an ASDEX SXR profile based on $M=0$ to $M=5$.

